

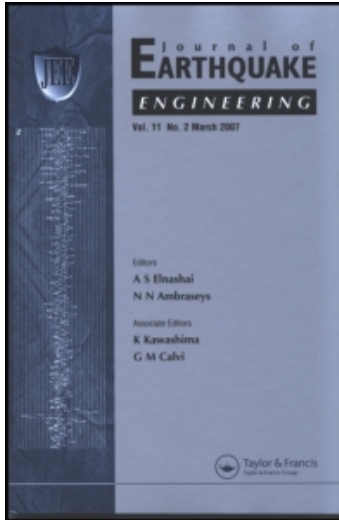
This article was downloaded by: [CDL Journals Account]

On: 15 December 2010

Access details: Access Details: [subscription number 922973516]

Publisher Taylor & Francis

Informa Ltd Registered in England and Wales Registered Number: 1072954 Registered office: Mortimer House, 37-41 Mortimer Street, London W1T 3JH, UK



Journal of Earthquake Engineering

Publication details, including instructions for authors and subscription information:

<http://www.informaworld.com/smpp/title~content=t741771161>

Experimental and Numerical Seismic Response of a 65 kW Wind Turbine

Ian Prowell^a; Marc Veletzos^b; Ahmed Elgamal^a; José Restrepo^a

^a Department of Structural Engineering, University of California, San Diego, La Jolla, California, USA ^b

Department of Civil Engineering, Merrimack College, North Andover, Massachusetts, USA

To cite this Article Prowell, Ian , Veletzos, Marc , Elgamal, Ahmed and Restrepo, José(2009) 'Experimental and Numerical Seismic Response of a 65 kW Wind Turbine', Journal of Earthquake Engineering, 13: 8, 1172 – 1190

To link to this Article: DOI: 10.1080/13632460902898324

URL: <http://dx.doi.org/10.1080/13632460902898324>

PLEASE SCROLL DOWN FOR ARTICLE

Full terms and conditions of use: <http://www.informaworld.com/terms-and-conditions-of-access.pdf>

This article may be used for research, teaching and private study purposes. Any substantial or systematic reproduction, re-distribution, re-selling, loan or sub-licensing, systematic supply or distribution in any form to anyone is expressly forbidden.

The publisher does not give any warranty express or implied or make any representation that the contents will be complete or accurate or up to date. The accuracy of any instructions, formulae and drug doses should be independently verified with primary sources. The publisher shall not be liable for any loss, actions, claims, proceedings, demand or costs or damages whatsoever or howsoever caused arising directly or indirectly in connection with or arising out of the use of this material.

Experimental and Numerical Seismic Response of a 65 kW Wind Turbine

IAN PROWELL¹, MARC VELETZOS², AHMED ELGAMAL¹,
and JOSÉ RESTREPO¹

¹Department of Structural Engineering, University of California, San Diego,
La Jolla, California, USA

²Department of Civil Engineering, Merrimack College, North Andover,
Massachusetts, USA

A full-scale shake table test is conducted to assess the seismic response characteristics of a 23 m high wind turbine. Details of the experimental setup and the recorded dynamic response are presented. Based on the test results, two calibrated beam-column finite element models are developed and their characteristics compared. The first model consists of a vertical column of elements with a lumped mass at the top that accounts for the nacelle and the rotor. Additional beam-column elements are included in the second model to explicitly represent the geometric configuration of the nacelle and the rotor. For the tested turbine, the experimental and numerical results show that the beam-column models provide useful insights. Using this approach, the effect of first-mode viscous damping on seismic response is studied, with observed experimental values in the range of 0.5–1.0% and widely varying literature counterparts of 0.5–5.0%. Depending on the employed base seismic excitation, damping may have a significant influence, reinforcing the importance of more accurate assessments of this parameter in future studies. The experimental and modeling results also support earlier observations related to the significance of higher modes, particularly for the current generation of taller turbines. Finally, based on the outcomes of this study, a number of additional experimental research directions are discussed.

Keywords Renewable Energy; Green Energy; Earthquake; Seismic; Shake Table; Wind Turbine

1. Introduction

The wind industry continues to grow rapidly throughout the world with almost 20 GW of capacity erected in 2007 and total production rapidly approaching 100 GW worldwide [DOE, 2008]. Over one quarter of the turbines installed in 2007 reside in the United States (US), India, and China [DOE, 2008], all with large regions of high seismic hazard. Accordingly, seismic provisions were recently added to wind turbine certification guidelines [GL, 2003; IEC, 2005].

The growth of wind turbine installations has led to an increased interest in addressing the related seismic loading considerations. Early investigations [Bazeos *et al.*, 2002; Lavassas *et al.*, 2003] focused on the tower, using models that lumped the nacelle and rotor as a point mass (Fig. 1). Detailed shell-element models were developed to investigate the tower stresses and potential load concentration/buckling scenarios. Bazeos *et al.* [2002] also provided a thorough comparison of dynamic response, employing a full shell-element, a simpler beam-column, and a single-degree-of-freedom model approach.

Received 11 March 2009; accepted 14 March 2009.

Address correspondence to Ahmed Elgamal, Department of Structural Engineering, University of California, San Diego, La Jolla, California 92093-0085, USA; E-mail: elgamal@ucsd.edu

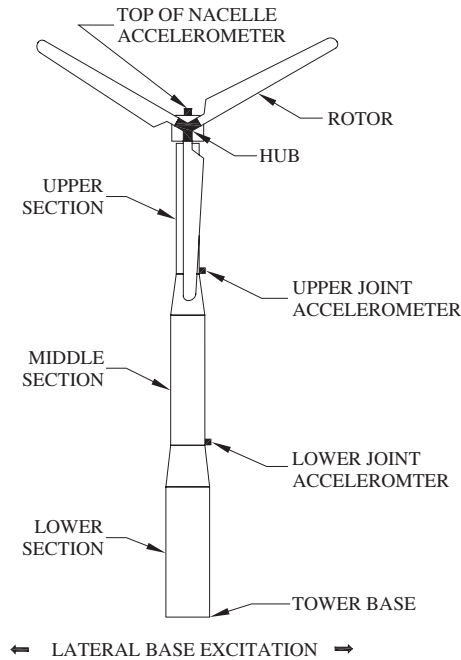


FIGURE 1 Wind turbine configuration and location of accelerometers.

More recent work [Ritschel *et al.*, 2003; Witcher, 2005; Haenler *et al.*, 2006] used models that explicitly simulate the rotor (Figure 1) along with the turbine tower. In addition, equivalent springs and dampers were included at the model base to simulate the effects of soil structure interaction [Bazeos *et al.*, 2002; Zhao and Maissner, 2006]. A comprehensive review of existing literature has been recently compiled by Prowell and Veers [2009], along with a simplified seismic demand assessment approach for tower heights ranging from 24 m (50 kW) to 90 m (5 MW).

Recognizing that experimental validation is currently scarce, a full scale test was planned and conducted at the University of California, San Diego (UCSD). An actual 65 kW wind turbine was subjected to base excitation using the Network for Earthquake Engineering Simulation (NEES) Large High Performance Outdoor Shake Table (LHPOST). This experiment provided a baseline for seismic behavior of a parked turbine in low winds. Analysis of the experimental results was conducted to infer natural frequencies, mode shapes, and equivalent viscous damping. These results were then employed to calibrate two simple finite element (FE) models that may be of use for conducting practical analyses [Agbayani, 2002; Bazeos *et al.*, 2002; Lavassas *et al.*, 2003; Jonkman and Buhl, 2005; Witcher, 2005; Haenler *et al.*, 2006].

The numerically derived modal properties were compared to those observed experimentally. Following calibration, the model that explicitly represents the rotor blades was used to conduct numerical simulations. For that purpose, a suite of California earthquake records was employed as base input excitation. The influence of equivalent viscous damping on the predicted turbine response was assessed. Finally, the reported results were used to motivate future research into the dynamics of wind turbines under earthquake loading conditions.

2. Shake Table Experiment

A full-scale test was conducted at UCSD to explore the response of a parked turbine due to base excitation. For that purpose, Oak-Creek Energy Systems of Mojave, California donated a 65 kW turbine that was erected on site and mounted on the shake table platform (Fig. 2).

2.1. Turbine Description

The tested 65 kW turbine (Fig. 2) was manufactured in Denmark by Nordtank. In the early 1980s, this Nordtank turbine and its contemporaries were installed in large numbers for utility scale power generation in California [Hau, 2006]. By 1985, Danish machines accounted for approximately 40% [Hau, 2006] of the turbines installed throughout California (Fig. 3).

These early turbines are often employed beyond the original design life, with retired machines frequently sold on the secondhand market [Burns, 2009]. In comparison to modern Megawatt-level machines, the tested unit is relatively small, but represents the canonical configuration (Fig. 1) of a tubular steel tower topped with a nacelle that actively yaws to orient the rotor into the wind. A summary of the pertinent engineering properties of the test turbine is presented in Table 1.

2.2. Shake Table Facility

The LHPOST [Restrepo *et al.*, 2005] was built to impart uni-axial horizontal excitation, with a platform of 7.6 m by 12.2 m in size (Fig. 2) and a stroke of ± 0.75 m. Salient features include a peak horizontal velocity of 1.8 m/s, a horizontal force capacity of

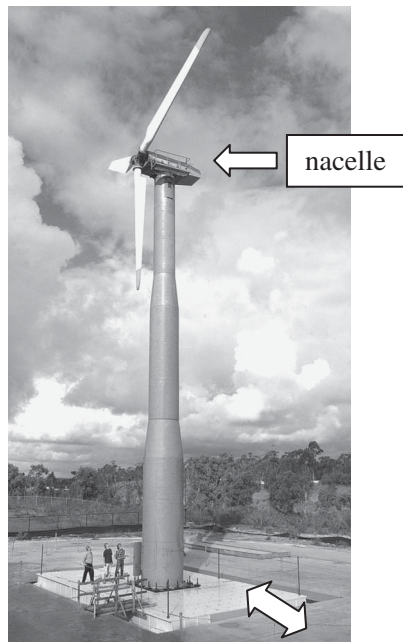


FIGURE 2 Wind turbine mounted on the outdoor UCSD shake table.



FIGURE 3 Field installation at Oak Creek Energy Systems in Tehachapi, CA.

TABLE 1 Properties of the 65 kW wind turbine

Property	Value
Rated power	65 kW
Rated wind speed	34 km/H (21 MPH)
Rotor diameter	16.0 m (628 inches)
Tower height	21.9 m (864 inches)
Lower section length	7.96 m (313 inches)
Lower section diameter	2.02 m (78 inches)
Middle section length	7.94 m (312 inches)
Middle section diameter	1.58 m (62 inches)
Top section length	6.05 m (238 inches)
Top section diameter	1.06 m (41 inches)
Tower wall thickness	5.3 mm (0.20 inches)
Rotor hub height	22.6 m (888 inches)
Tower mass	6400 kg (14 kips)
Nacelle mass	2400 kg (5 kips)
Rotor mass (with hub)	1900 kg (4 kips)

6.8 MN, and a vertical peak payload capacity of 20 MN. The overturning moment capacity is 50 MN-m (for a nominal specimen configuration with mass = 200 metric tons at an effective height of 10 m, and acceleration = 2.5 g). Motions containing frequencies up to 33 Hz can be simulated. These characteristics make the LHPOST the largest seismic shake table worldwide in terms of load capacity and the first outdoor facility of its kind. The LHPOST adds a significant new capability to U.S. testing facilities, with no overhead space and lifting constraints, that being an essential consideration for full scale wind turbine experimentation.

2.3. Experimental Test Program

For all test motions, the rotor was parked with one blade oriented downward, parallel to the tower (Fig. 2). The uni-axial horizontal base motion was imparted in the lateral direction of the turbine, perpendicular to the rotor's axis of rotation (Fig. 2). To capture this lateral response, uni-axial DC-coupled accelerometers were installed as indicated in Fig. 1. One accelerometer was located on top of the shake table. Four others were located on the tower, at the base, the lower joint, the upper joint, and at the top of the nacelle (Fig. 1).

Excitation for the tests was derived from the East-West component (0.15 g Peak Ground Acceleration, PGA) of the June 28th, 1992 strike-slip Landers Earthquake (moment magnitude $M_w = 7.3$) recorded at Desert Hot Springs (DHS). DHS is a California Strong Motion Instrumentation Program station situated on deep alluvium, 23 km from the fault trace of the Landers Earthquake. With a shear wave velocity of 345 m/s at a depth of 30 m [CSMIP, 2006], the ground profile is classified as stiff soil, site class D [ASCE, 2005].

To remove any superfluous DC offset as well as high frequency noise, the original earthquake record was filtered with a band pass of 0.05–25 Hz. The record was then scaled to approximately 100%, 150%, and 200% of the original amplitude for the tests. Figure 4 and Fig. 5 present the recorded data for the 100% and 200% level tests, respectively. The above experimentation program constitutes the first full scale base excitation test of a wind turbine and to date is the tallest structure tested on a shake table.

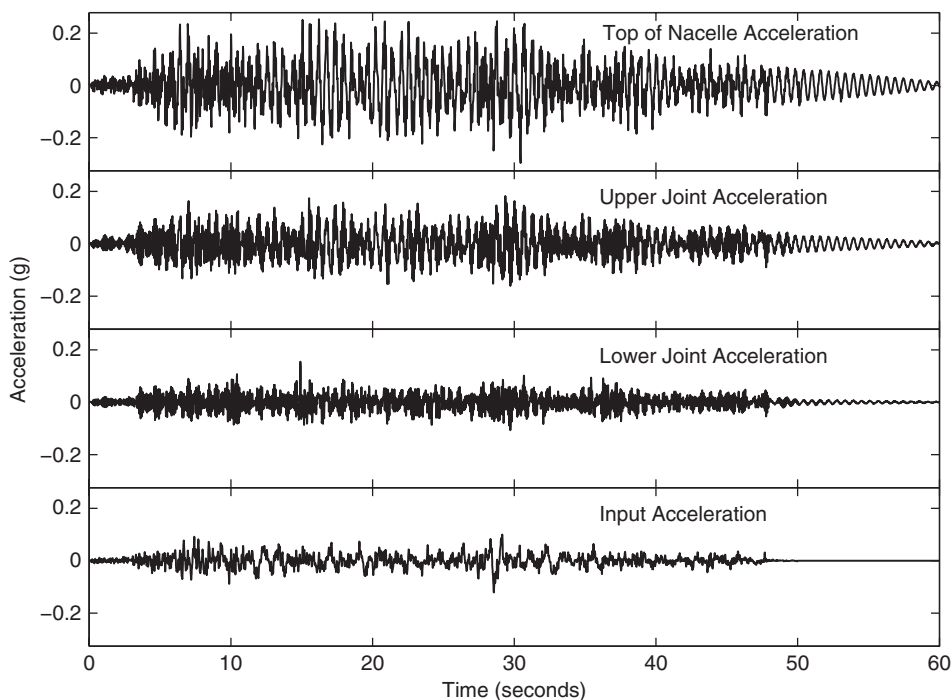


FIGURE 4 Recorded acceleration for Landers 100% level test.

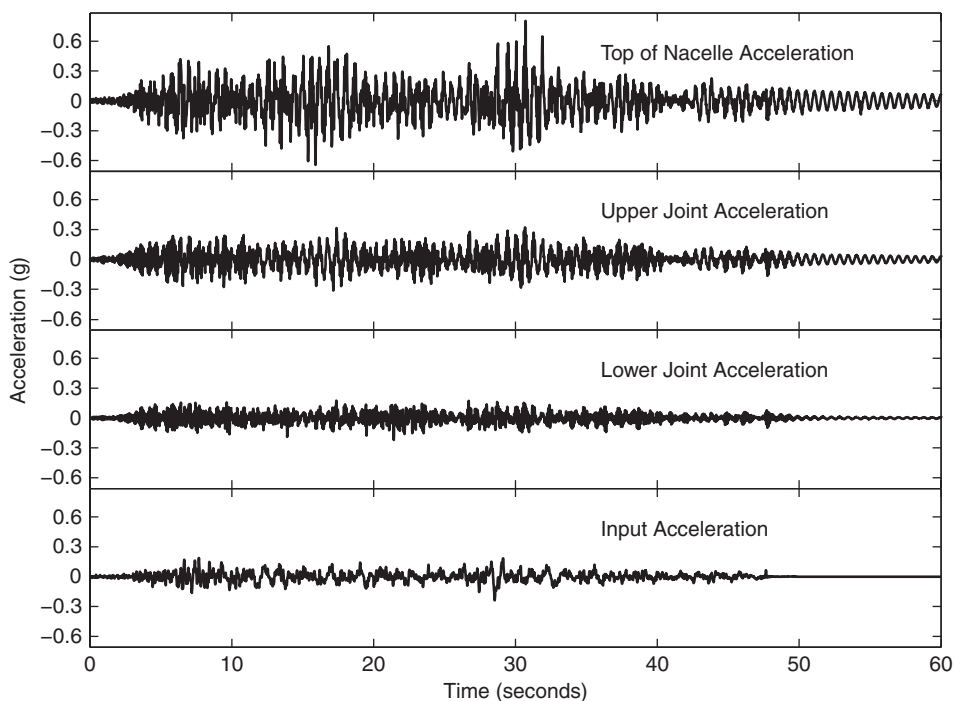


FIGURE 5 Recorded acceleration for Landers 200% level test.

2.4. Experimentally Observed Modal Properties

Natural frequencies and mode shapes were extracted from the experimentally observed data. As mentioned earlier, the deployed accelerometers (Fig. 1) only record the lateral component (in the direction of base shaking) of dynamic response. Figure 6 shows the calculated acceleration transfer function (base to top of the nacelle) for each of the base shaking tests. The results show good agreement (Fig. 6 and Fig. 7) with a consistent first natural frequency of about 1.7 Hz ($T = 0.6$ s), indicating an essentially linear response. A band of higher resonance appears around 11.7–12.3 Hz ($T = 0.08$ – 0.09 s), with agreement between the tests appearing to be somewhat lower (Fig. 6).

For each accelerometer location (Fig. 1), an average of the amplitude and phase of the transfer functions was used to construct mode shapes at the observed resonances. The fundamental mode shape (Fig. 8a) and that of a higher mode (Fig. 8b) are seen to resemble the bending modes of a cantilever beam with a point mass [Laura *et al.*, 1974].

Equivalent viscous damping during dynamic excitation is also a property of interest. Using the recorded time histories, the log decrement method [Chopra, 2006] was used to estimate damping at the first natural frequency. After the shaking phase, the higher resonances quickly decay, resulting in an essentially first mode free vibration response (48–60 s in Fig. 4 and Fig. 5).

On this basis, damping was estimated to be less than 1 percent (Table 2) at the first natural frequency. With quiescent winds and a parked rotor, damping within the turbine

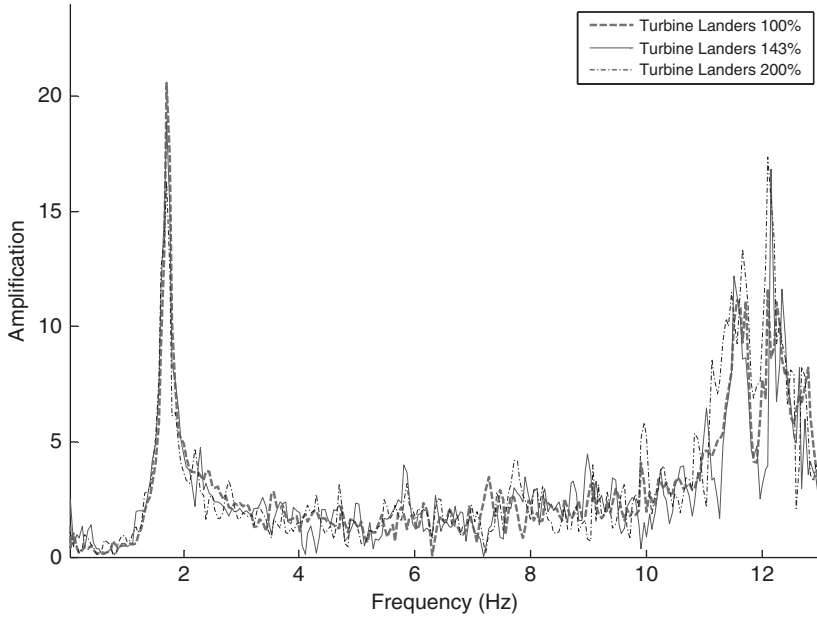


FIGURE 6 Recorded transfer function.

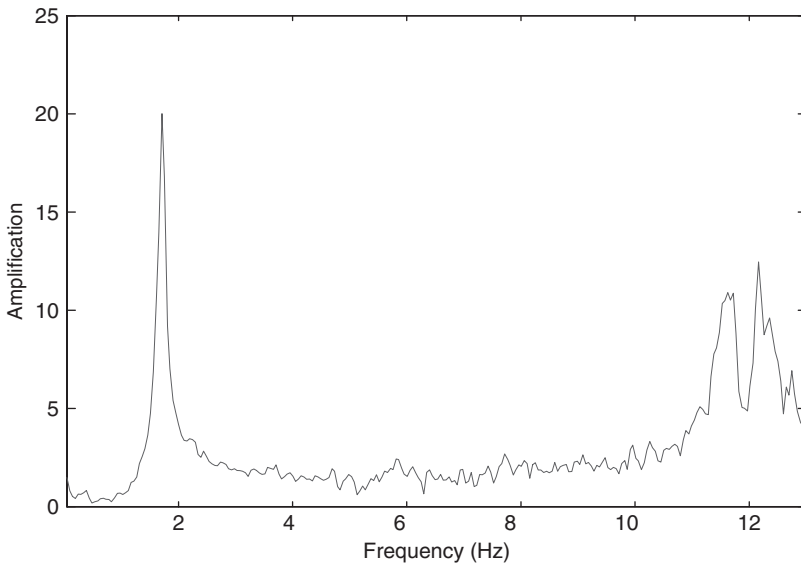


FIGURE 7 Average transfer function.

structure has likely dominated these observed low values (Table 2). It should be noted that in-situ values may in certain cases be higher, due to considerations such as energy radiation through the foundation [Kramer, 1996] and aeroelastic damping in both horizontal directions for an operating turbine [Riziotis *et al.*, 2004].

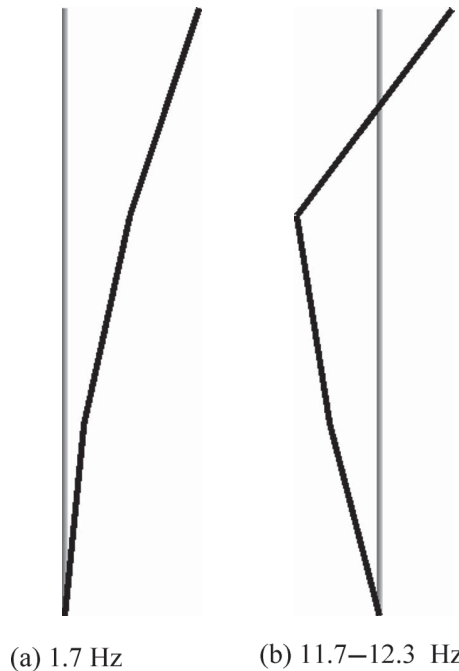


FIGURE 8 Experimentally observed lateral modes.

TABLE 2 Observed damping for Landers motion (logarithmic decrement method)

Approximate scaling	Average damping
100%	0.86%
150%	0.43%
200%	0.41%

3. Finite Element Modeling

Earlier results suggest that a beam-column model provides results that are consistent with more detailed shell models for towers [Bazeos *et al.*, 2002] as well as turbine blades [Malcolm and Laird, 2003]. On this basis, two simple FE models were studied herein. The first (Model I) consisted of a cantilever beam with distributed tower mass and an additional lumped mass at the top to represent the nacelle and rotor [Bazeos *et al.*, 2002; Lavassas *et al.*, 2003]. The second (Model II), explicitly represented the turbine’s geometric configuration and mass distribution by adding beam-column elements to emulate the nacelle and rotor [Witcher, 2005; Haenler *et al.*, 2006]. Currently, these simple modeling configurations correspond to the two main approaches for simulation of seismic loading on wind turbines.

The above FE models were implemented using the open source computational platform OpenSees [Mazzoni *et al.*, 2006]. In both cases, the tower (Fig. 1) was divided into 30 beam-column elements with a flexural stiffness based on the cross section at the

center of each element. Model II was developed with 12 beam-column elements per blade to represent the mass and stiffness of the rotor (Fig. 1 and Fig. 2). A hinge condition was added to allow for the free rotation of the rotor. Finer meshes for the tower and blade were investigated, but the results were not significantly impacted by such refinement. The blade mass and stiffness distribution was approximated by scaling reported values for a similar unit [Jonkman and Buhl, 2005] to match the Nordtank blade geometry. Unlike the tower where bending stiffness at the base is only 8 times that of the upper section, the blade is over 3000 times stiffer at the root compared to the tip.

3.1. Finite Element Modal Properties

Based on the engineering properties (Table 1) and Young's Modulus for steel = 200 GPa, Model I (bending beam with a point mass) closely matched the experimentally observed first natural frequency (1.7 Hz) and mode shape (Fig. 9a). The second cantilever type mode occurred at 11.8 Hz, in the neighborhood of the higher experimentally observed resonance (Fig. 9b). At a much higher frequency (34.1 Hz), a third bending mode was predicted (Fig. 9c).

Model II with the explicit rotor representation also matched the first natural frequency and mode shape (Fig. 10). Due to the involved rotor eccentricity, Model II showed an additional longitudinal bending mode parallel to the rotor's axis rotation at 1.7 Hz (Fig. 11) and a first torsional mode at 9.2 Hz (Fig. 12). The next mode, a second cantilever type longitudinal mode, was observed at 9.7 Hz (Fig. 13). A second cantilever type lateral mode was then observed at 12.1 Hz (Fig. 14), within the range of the higher observed resonance. The third longitudinal bending mode in Model II was predicted at 21.5 Hz (Fig. 15), which is a much lower frequency than the prediction for Model I.

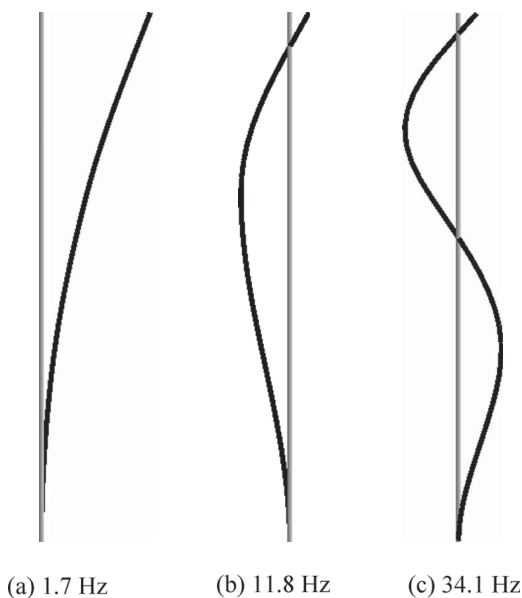


FIGURE 9 Model I OpenSees lateral modes.

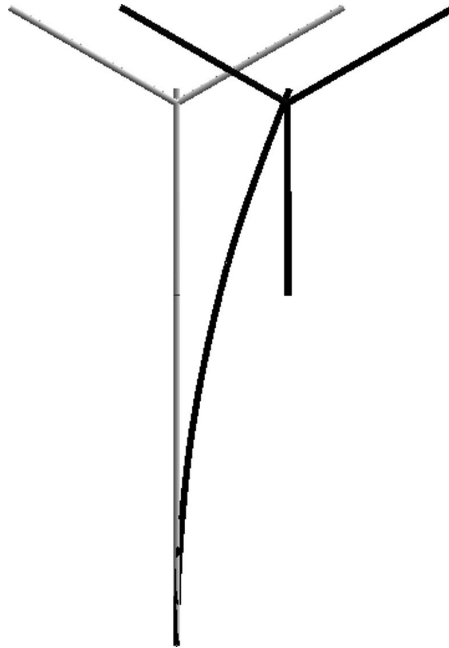


FIGURE 10 OpenSees Model II 1st lateral mode (1.7 Hz).

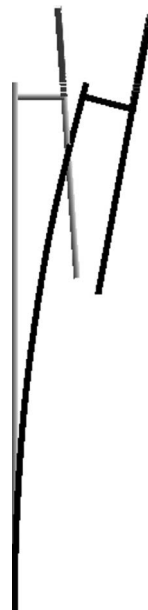


FIGURE 11 OpenSees Model II 1st longitudinal mode (1.7 Hz).

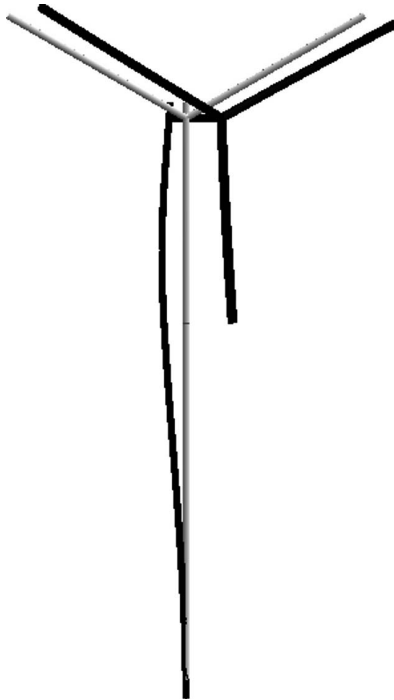


FIGURE 12 OpenSees Model II 1st torsional mode (9.2 Hz).



FIGURE 13 OpenSees Model II 2nd longitudinal mode (9.7 Hz).



FIGURE 14 OpenSees Model II 2nd lateral mode (12.1 Hz).



FIGURE 15 OpenSees Model II 3rd longitudinal mode (21.5 Hz).

As such, both models showed reasonable results for the first and second observed lateral bending modes. This reasonable agreement reinforces earlier observations as to the viability of simple models for predicting seismic response (for the tested turbine). While outside the range of seismic excitation, Models I and II predicted significantly different resonant frequencies for the third tower bending mode (Fig. 9c and Fig. 15). For modern large turbines, such higher bending modes may well fall within the seismic range of interest [Haenler *et al.*, 2006], possibly highlighting the need for further modeling refinements.

4. Numerical Simulation of Recorded Response

Model II with the explicit rotor representation, was used to conduct dynamic base excitation simulations. Based on the recorded response and industry guidelines [IEC, 2005], damping was set to 1% for the first mode. At the higher resonance band (near 12 Hz), a value of 3.5% was needed for a better match with the recorded response (specified in the form of Rayleigh damping). Figure 16 and Fig. 17 show a comparison of the recorded and simulated time histories (100% and 200%, respectively) for the calibrated model. This good agreement between observed and computed response, was found to hold for any first mode damping within the experimentally observed range of about 0.5–1% (Table 2).

5. Numerical Modeling of Seismic Response

After calibration, Model II simulations were conducted using a set of ground motions from California earthquakes (Table 3). These motions were all recorded at ground level

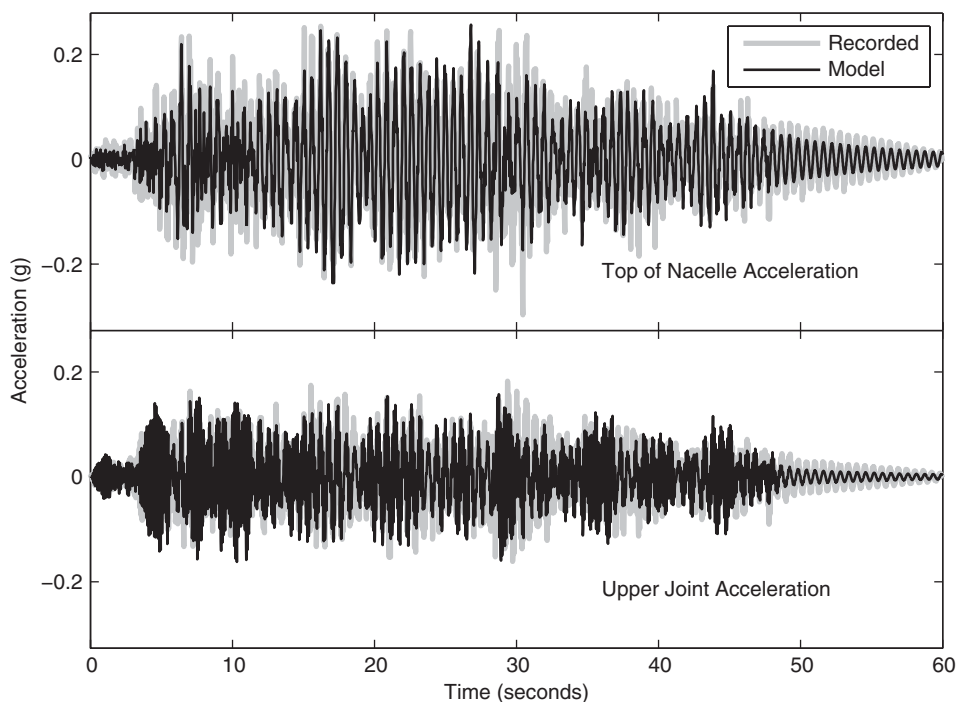


FIGURE 16 Model II acceleration for Landers 100% level simulation.

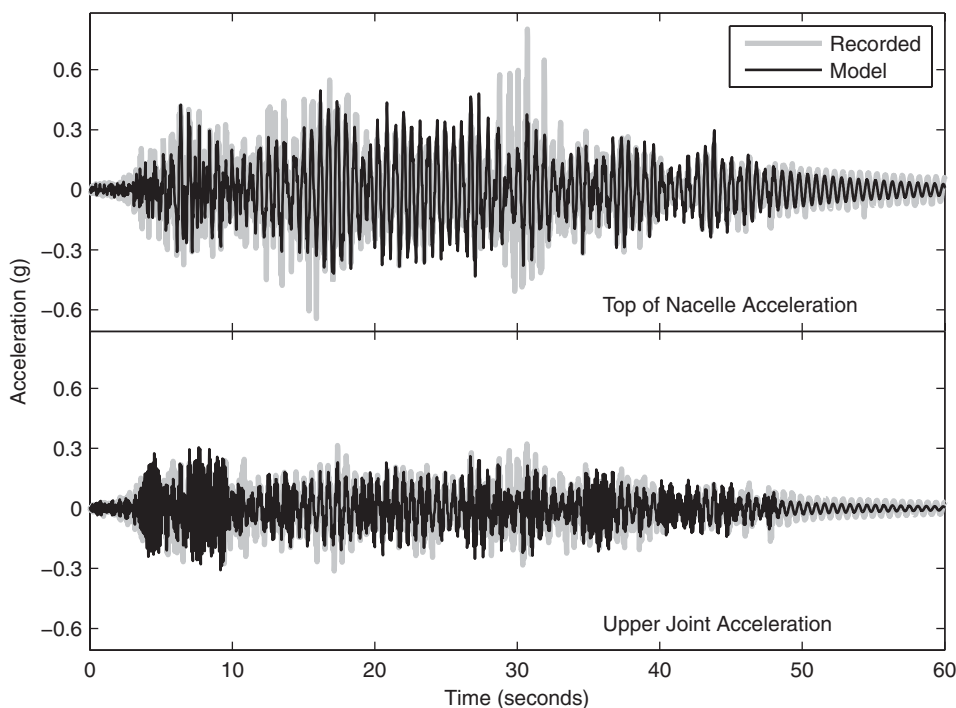


FIGURE 17 Model II acceleration for Landers 200% level simulation.

TABLE 3 Earthquake data

Earthquake	Moment magnitude (M_w)	Station	PGA (g)
1940 El Centro 180°	6.9	Array Station 9	0.35
1979 Coyote Lake 230°	5.7	Gilroy Array Station 6	0.42
1986 Palm Springs 0°	6.2	New Fire Station	0.33
2000 Yountville 90°	5.0	Fire Station No. 3	0.41

in relatively stiff structures (one or two story buildings). For reference, the IBC design spectrum (ICC 2006) for DHS is seen to be an envelope around the selected motion spectra (Fig. 18).

As in the shake table test, excitation was imparted laterally. In light of certification guidelines [GL, 2003; IEC, 2005] and the observed behavior, linear response was studied without consideration of potential shell buckling or other nonlinear phenomena (which should be carefully analyzed if deemed necessary).

Influence of damping on seismic response was investigated. For that purpose, base excitation (Fig. 19) was simulated using 0.5% [Bazeos *et al.*, 2002], 1% [IEC, 2005], 2% [Agbayani, 2002], and 5% [ICC, 2006] of critical damping at the first resonance. At the higher resonance range damping was kept constant at 3.5%. As seen in Table 4, damping was of relatively little influence on peak acceleration in most cases. In contrast, the Palm Springs record showed a difference of about 100%. Figure 19 shows a comparison of the acceleration time histories at the top of the nacelle for the 0.5% and 5.0% damped scenarios. A clear difference may be seen (Fig. 19) in terms of the especially long duration of cyclic response for the 0.5% damping case.

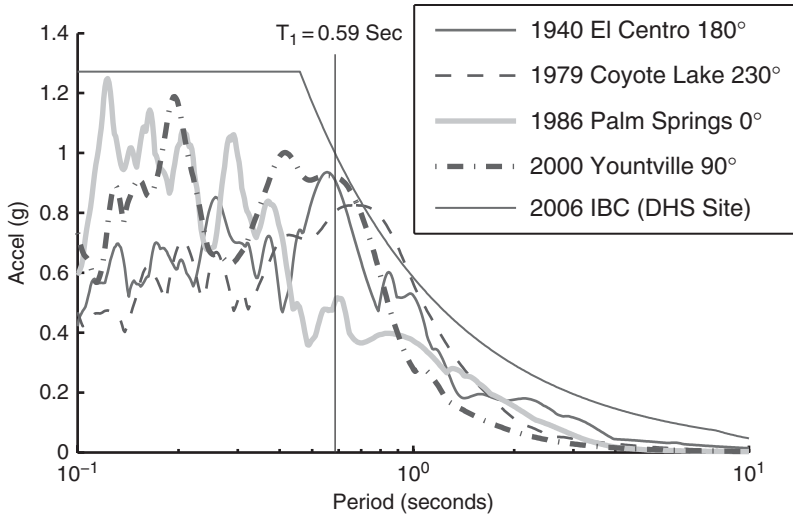


FIGURE 18 Comparison of 2006 IBC design spectrum to 5% damped elastic response spectrum at desert hot springs.

TABLE 4 Response at top of nacelle for different damping levels

Earthquake	Peak acceleration at top of nacelle (g)			
	5% Damped	2% Damped	1% Damped	0.5% Damped
1940 El Centro 180°	1.2	1.4	1.4	1.5
1979 Coyote Lake 230°	1.1	1.1	1.2	1.2
1986 Palm Springs 0°	0.8	1.1	1.3	1.6
2000 Yountville 90°	1.4	1.5	1.6	1.6

6. First Mode and Response Spectrum Seismic Response

Using modal analysis [Chopra, 2006], the following single-degree-of-freedom solution describes the turbine's first mode seismic response:

$$u = \phi_1 q_1 \quad (1)$$

$$\ddot{q}_1 + 2\zeta_1 \omega_1 \dot{q}_1 + \omega_1^2 q_1 = -\Gamma_1 \ddot{u}_g, \quad (2)$$

where u is the turbine displacement relative to the ground, the "1" subscript denotes first mode response, ϕ the mode shape, q the generalized coordinate, ω the resonant frequency in radians/second, ζ the viscous damping ratio, Γ the modal participation factor, and \ddot{u}_g is time history of the input seismic base acceleration.

With the parameters derived from Model II, the above equations were used to compute the turbine's seismic response to the input earthquake records of Table 4. In all cases, the results were quite close to those reported earlier using the FE beam-column Model II (Fig. 19). As such, the turbine's response at the nacelle level may be

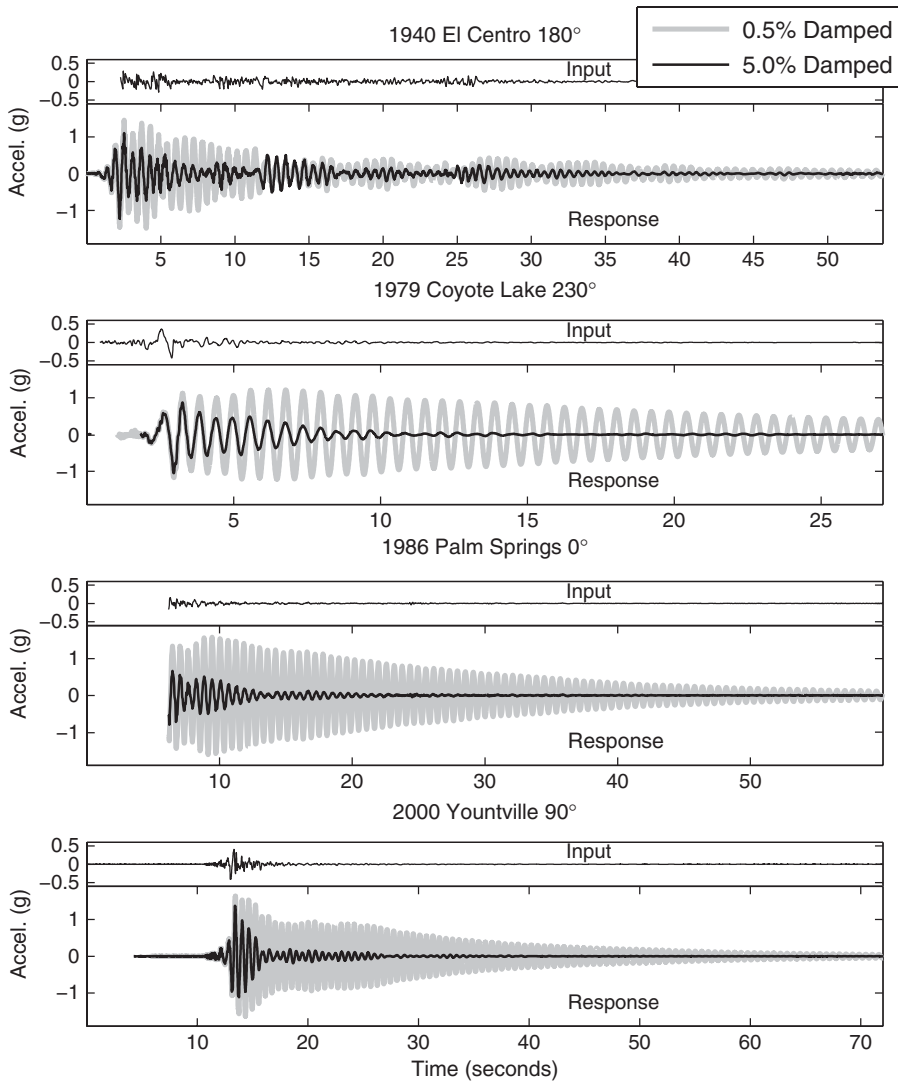


FIGURE 19 Input time history of ground motions and response at top of nacelle.

conveniently calculated using Eqs. (1) and (2), where $\Gamma = 1.2$ for a normalized modal value of 1.0 at this location. For units similar to the tested turbine, this simple approach may prove useful, in conjunction with the existing tools for estimation of wind turbine mode shapes [Bir, 2005].

Alternatively, an estimate of peak acceleration, a_{max} , at the nacelle may be obtained from the response spectrum of an earthquake record, that being equal to $1.2 S_a$ (where S_a is spectral acceleration at the fundamental period). The maximum moment may be estimated (Annex C of IEC, 2005) as $M_{max} = h_t \cdot a_{max} \cdot m_{eff}$ where m_{eff} , the effective mass, is equal to the mass of rotor, nacelle, and $\frac{1}{2}$ the tower and h_t is the tower height. The moment at any height, h , along the tower can be approximated as $M(h) = (h_t - h) \cdot a_{max} \cdot m_{eff}$ assuming linear variation. This implies a constant shear of $a_{max} \cdot m_{eff}$ throughout the tower.

7. Discussion of Results

The experimental and numerical results presented above suggest the following observations:

- i) For estimating the fundamental period, both employed FE models resulted in reliable predictions. Using the hub height plus 2/3 of the blade length, the 2006 IBC code estimate (see Appendix) closely agrees with both models and observation.
- ii) For units similar to the tested turbine, the results show seismic response to be governed primarily by the first mode. For such systems, a Rayleigh-Ritz approach based on the first mode shape yields a satisfactorily estimate of the system response.
- iii) Agreement between observations and numerical prediction was somewhat lower for the high frequency second lateral bending mode (around 10 Hz). However, as discussed earlier, this issue had no appreciable impact the conducted simulation results.
- iv) Seismic excitation records with especially high frequency content, may provoke higher mode behavior (e.g., the 1988 Saguenay earthquake record; Somerville *et al.* [1990]). For the new taller turbines, such modes will fall in the range of interest for earthquake loading [Haenler *et al.*, 2006]. Similar to most ground motion records in California, the employed test motion was relatively poor in high frequency energy. Future tests should be designed to include complementary shaking scenarios with low and high frequency content.
- v) Model II showed an offset in frequency between the second bending modes in the two horizontal directions as predicted earlier by Zhao *et al.* [2007]. Further tests with a denser configuration of multi-axial accelerometers are needed to more comprehensively document this type of higher frequency behavior.
- vi) Free vibration results show that a low level of damping (less than 1%) is not over conservative for modeling at the first natural frequency. This level is appropriate for the tested parked turbine scenario. Depending on the underlying ground properties, SSI may increase overall damping due to energy radiation [Kramer, 1996]. In addition, effective damping in both horizontal directions, for an operational turbine may be strongly influenced by wind speed [Riziotis *et al.*, 2004].

8. Research Directions

Further experimental and analytical research will provide valuable insights in important areas such as:

- i) In-situ vibration measurements for evaluation of system response including soil-structure interaction, and effective damping under parked and operating turbine conditions.
- ii) Full-scale shake-table experiments and associated modeling with the aim of assessing nonlinear response, failure modes, and the tower moment capacity. Multi-axial base shaking (3-dimensional) would be more representative of the actual seismic situation.

- iii) Development of a probabilistic seismic risk analysis framework [Prowell, 2010], comprehensively addressing the main involved vulnerability scenarios [GL, 2003; IEC, 2005].

9. Summary and Conclusions

Experimental results from the first full-scale shake table test of a wind turbine were presented. The salient resonant response characteristics were identified. First mode damping was estimated to be below 1% for the tested parked-turbine configuration. Beam-column computational models were calibrated, and found to be a valuable tool for assessment of seismic response. For small utility scale turbines, a first mode response was shown to provide a reasonable approximation. As such, the response spectrum approach may provide a convenient approach for estimating the seismically induced peak shear force and moment.

For larger modern turbines, higher modes may play a prominent role in the overall seismic response. Higher fidelity modeling may be necessary for such situations [Haenler *et al.*, 2006]. Additional experimental data related to damping, and soil structure interaction effects would be also most worthwhile.

Acknowledgments

The authors extend their gratitude to all the organizations, corporations, and individuals who contributed to this investigation, and who fund this research (NSF grant No. CMMI0830422). Oak Creek Energy Systems (Hal Romanowitz and J. Edward Duggan) generously donated the 65 kW turbine for shake table testing and continues to assist in advancing this important area of research. To facilitate this research, Dr. Paul Veers and the Sandia National Laboratories Wind Energy Technology Department provided internship support, guidance, and advice.

References

- Agbayani, N. A. [2002] "Design challenges in international wind power projects: from foreign codes to computer coding in a small office setting," *71st Annual Structural Engineers Association of California (SEAOC) Convention*, Santa Barbara, CA, pp. 117–132.
- ASCE [2005] *Minimum Design Loads for Buildings And Other Structures*, American Society of Civil Engineers, New York.
- Bazeos, N., Hatzigeorgiou, G. D., Hondros, I. D., Karamaneas, H., Karabalis, D. L., and Beskos, D. E. [2002] "Static, seismic and stability analyses of a prototype wind turbine steel tower," *Engineering Structures* **24**(8), 1015–1025.
- Bir, G. S. [2005] *User's Guide to BModes; Software for Computing Rotating Beam Coupled Modes*, National Renewable Energy Laboratory, Golden, CO.
- Burns, M. [2009] Personal Communication, Oak Creek Energy Systems, Mojave, CA.
- Chopra, A. K. [2006] *Dynamics of Structures: Theory and Application to Earthquake Engineering*, Prentice-Hall, Upper Saddle River, NJ.
- CSMIP [2006] "GR12149.htm: Station selected," available from <http://www.quake.ca.gov/cisn-edc/GrndResponsePages/GR12149.HTM> (accessed February 4, 2009).
- DOE [2008] *Annual Report on U.S. Wind Power Installation, Costs, and Performance Trends: 2007*, Department of Energy, Washington, D.C.
- GL [2003] *Guideline for the Certification of Wind Turbines*, Germanischer Lloyd, Hamburg, Germany.

- Haenler, M., Ritschel, U., and Warnke, I. [2006] "Systematic modelling of wind turbine dynamics and earthquake loads on wind turbines," *European Wind Energy Conference and Exhibition*, European Wind Energy Association, Athens, Greece, pp. 1–6.
- Hau, E. [2006] *Wind Turbines*, Springer-Verlag, New York.
- ICC [2006] *International Building Code 2006*, International Code Council, Country Club Hills, IL.
- IEC [2005] *IEC 61400-1 Ed.3: Wind turbines - Part 1: Design requirements*, International Electrotechnical Commission, Geneva, Switzerland.
- Jonkman, J. M. and Buhl, M. L., Jr. [2005] "*FAST User's Guide*," *Rep. No. NREL/EL-500-38230*, National Renewable Energy Laboratory, Golden, CO.
- Kramer, S. L. [1996] *Geotechnical Earthquake Engineering*, Prentice-Hall, Upper Saddle River, NJ.
- Laura, P. A. A., Pombo, J. L., and Susemihl, E. A. [1974] "A note on the vibrations of a clamped-free beam with a mass at the free end," *Journal of Sound Vibration* **37**(2), 161–168.
- Lavassas, I., Nikolaidis, G., Zervas, P., Efthimiou, E., Doudoumis, I. N., and Baniotopoulos, C. C. [2003] "Analysis and design of the prototype of a steel 1-MW wind turbine tower," *Engineering Structures* **25**(8), 1097–1106.
- Malcolm, J. D. and Laird, D. L. [2003] "Modeling of blades as equivalent beams for aeroelastic analysis," *2003 ASME Wind Energy Symposium AIAA/ASME*, Reno, NV, pp. 293–303.
- Mazzoni, S., McKenna, F., and Fenves, G. L. [2006] *Open System for Earthquake Engineering Simulation User Manual*, Pacific Earthquake Engineering Research Center, University of California, Berkeley, CA.
- Prowell, I. and Veers, P. [2009] "Assessment of wind turbine seismic risk: existing literature and simple study of tower moment demand," *Rep. No. SAND2009-XXXX (to be published)*, Sandia National Laboratories, Albuquerque, NM.
- Prowell, I. [2010] "A seismic study of wind turbines for renewable energy," PhD thesis, University of California, San Diego, La Jolla, CA.
- Restrepo, J. I., Conte, J. P., Enrique, L., J., Seible, F., and Van Den Einde, L. [2005] "The NEES@UCSD large high performance outdoor shake table earthquake engineering and soil dynamics (GSP 133)," *Proc. Geo-Frontiers 2005, Sessions of the Geo-Frontiers 2005 Congress*, Austin, TX.
- Ritschel, U., Warnke, I., Kirchner, J., and Meussen, B. [2003] "Wind turbines and earthquakes," *2nd World Wind Energy Conference*, World Wind Energy Association, Cape Town, South Africa.
- Riziotis, V. A., Voutsinas, S. G., Politis, E. S., and Chaviaropoulos, P. K. [2004] "Aeroelastic stability of wind turbines: the problem, the methods and the issues," *Wind Energy* **7**(4), 373–392.
- Somerville, P. G., McLaren, J. P., Saikia, C. K., and Helmberger, D. V. [1990] "The 25 November 1988 Saguenay, Quebec, earthquake: Source parameters and the attenuation of strong ground motion," *Bulletin of the Seismological Society of America* **8**(5), 1118–1143.
- Witcher, D. [2005] "Seismic analysis of wind turbines in the time domain," *Wind Energy* **8**(1), 81–91.
- Zhao, X. and Maissner, P. [2006] "Seismic response analysis of wind turbine towers including soil-structure interaction," *Proc. of the Institution of Mechanical Engineers, Part K: Journal of Multi-Body Dynamics* **220**(1), 53–61.
- Zhao, X., Maissner, P., and Jingyan, W. [2007] "A new multibody modeling methodology for wind turbine structures using a cardanic joint beam element," *Renewable Energy* **32**(3), 532–546.

Appendix: Code Based Estimate of Fundamental Period

For the 2006 IBC [ICC, 2006], the turbine's fundamental period T (in seconds) is estimated by the equation $T = C_t(h_n)^x$, in which h_n is height, and C_t and x are constants with the default values of 0.0488 and 0.75 (metric units), respectively. In order to match the observed period T of 0.59 s, an effective turbine height $h_n = 27.8$ m is needed, approximately equal to the turbine hub height of 22.6 m plus two thirds of the blade length. This effective height implicitly accounts for the geometric configuration of the rotor blades extending above the turbine's tower (Figure 1 and Figure 2).